EVLA Memo 118

Ionospheric Effects and Imaging and Calibration of VLA Data

W. D. Cotton

Abstract

Ionospheric electron density variations cause a time and position variable refraction of sources seen through the medium. In extreme cases, i.e. AT low frequencies, this can also defocus the image of the sky. The field–based technique of [2], [1] developed for use at 74 MHz is described with recent enhancements of low frequency techniques as implemented in Obit.

Contents

List of Figures

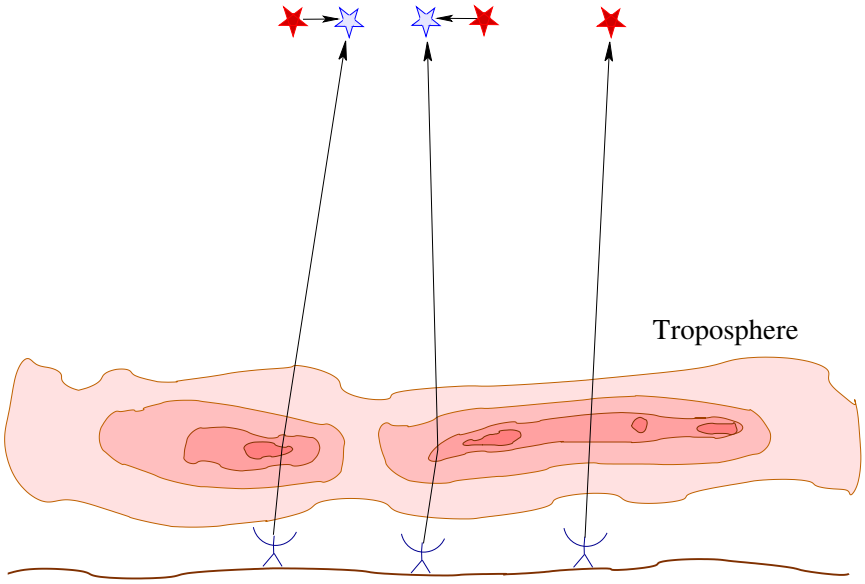

Figure 1.1: A cartoon view of the troposphere over an interferometer array. The shading shows the relative index of refraction and the lines show the effects on the apparent direction to the source. The tropospheric refraction causes relatively independent apparent deflections of source positions among the various antennas. Since the phase screen is so close to each antenna, a large area of the sky is viewed through the same portion of the phase screen.

1.1 Introduction

Electromagnetic signals propagating through an ionized medium experience an excess phase delay proportional to the frequency to the -2 power and can be a serious source of phase corruptions for radiation at low frequencies. The Earth's ionosphere is such an ionized medium and its irregularities have long been recognized as the major source of phase errors for high resolution arrays at frequencies below ∼100 MHz. However, since the resolution of an array is proportional to the frequency, the effects of ionospheric phase corruptions on derived images only drop as the frequency to the negative first power.

This document describes the current state of the development of the techniques. All data manipulation discussed in this report use the Obit package (http://www.cv.nrao.edu/∼bcotton/Obit.html) and plots were generated in AIPS. A related discussion can be found in [3].

1.2 Field–Based Calibration

An electromagnetic wavefront passing through a medium of variable index of refraction will experience variable phase delays in different parts of the wavefront. A wedge in the density of such a medium will cause a linear gradient across an array observing through such a medium resulting in a refraction of any objects viewed. Higher order variations in the index of refraction will cause a more serious distortion of the wavefront producing defocusing and scintillations in extreme cases. Calibration of interferometric arrays involves estimating and correcting these phase effects.

The traditional antenna–based calibration is designed to model phase corruptions largely due to variations in tropospheric water vapor density fluctuations. This case is illustrated in cartoon form in Figure 1.1 where it is seen that the phase screen is quite close to the antennas so that the phase errors are largely uncorrelated between antennas. Also, since the phase screen is so close to the antenna, the phase errors at each antenna will be correlated over large areas of the sky. Thus, a single phase per antenna suffices to describe the tropospheric phase corruptions.

On the other hand, the ionosphere is at a much greater height, from about 100 km to several hundred km and is illustrated in the cartoon Figure 1.2. In this case, the phase corruptions are

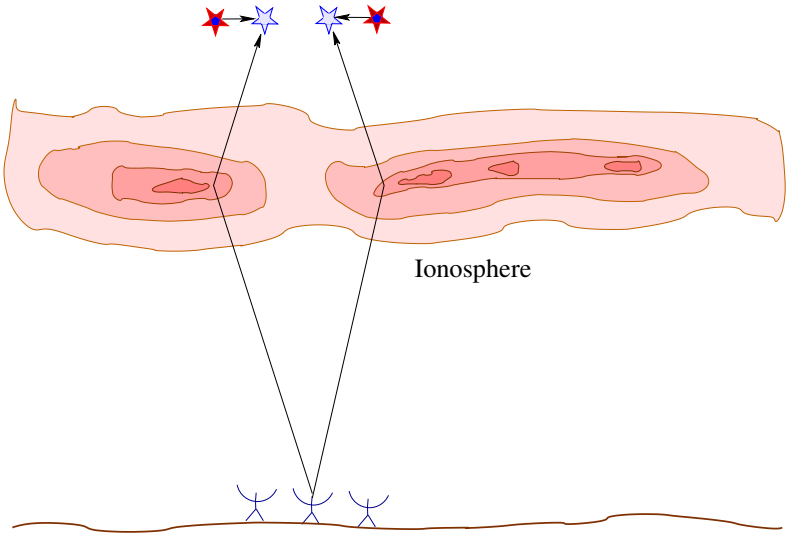

Figure 1.2: A cartoon view of the ionosphere over a telescope array. The shading shows relative values of the index of refraction and the lines show the effects on the apparent direction to the source. Each element of the array looks through nearly the same portion of the ionosphere towards a given source but the portion of the ionosphere varies between sources.

highly correlated between antennas but vary with angle on the sky. Thus, the "isoplanatic" patch size may be smaller than in the case of tropospheric phase errors. Ionospheric phase errors are not well described by a single phase per antenna but are better described by a phase screen across the array.

In the regime that the phase screen can be adequately described as a linear gradient across the array for a wavefront coming from any given direction, the image of a small source will not be distorted or defocused, but will appear shifted from its actual position. This apparent position shift may vary across the field of view of the array elements. In this regime, the "field–based" method of [2], [1] is applicable. This technique is to make a series of snapshot measurements around the locations of known strong sources in the field, deconvolve the images, and estimate the apparent offsets of each. The time sequence of the derived set of apparent source position offsets allows the fitting of a time variable geometric distortion of the sky as seen by the array. Low order Zernike polynomials are a useful function for modeling the distortion field. The field is modeled as a phase screen and each position offset measurement gives a 2-D gradient in this screen at the puncture point of the line of sight to the calibrator. Due to the paucity of usable calibrators in VLA 74 MHz observations, only a 5 term Zernike model is used. This allows a 2D gradient in position offsets across the field of view. There is no simple operation that can "calibrate" the data due to the spatial dependence of the correction. The time variable geometric distortion model must be used in the imaging and deconvolution process to apply corrections.

At low frequencies with 2-D arrays, some provision must be made for the curvature of the sky. One solution to this problem is the "Fly's eye" approach where the sky is tiled with many small facets each tangent to the celestial sphere at its center. In practice, the size of the tile needed is smaller than the isoplanatic patch size (or at least the resolution at which the phase screen can be determined), so a sufficient approximation to dedistorting the sky is to correct each facet for the ionospheric offset at its center. This is done by calculating the antenna-based phase corrections at the center of the facet and applying these corrections prior to deriving the dirty image (or residual) of that facet. If a visibility based deconvolution is used, the apparent positions of the CLEAN components need time dependent corrections, before Fourier transforming, to reintroduce the distortions into the model.

1.2.1 Calibrator Catalog

The process of estimating the distortion field in each time segment requires a good catalog of strong sources. The wide area surveys suitable for this, NVSS, WENSS, SUMSS are at higher frequencies and possibly lower resolution than the frequency and resolution of the data to be calibrated. The cataloged position of sources may not correspond to the centroid at the frequency being observed. Furthermore, not all sources are equally useful for position offset measurements, resolved sources may have a relatively poorly defined centroid, especially when viewed with a very elongated beam at low elevations. The best calibrators are unresolved and isolated. However, bright but complex sources must be included in the snapshot deconvolutions since the poor uv-coverage will result in widespread side-lobes. The calibrator catalog must therefore contain all bright sources with an indication of the usability of each entry, ie. an indication of crowding. For the best calibration, it may be necessary to derive the source catalog from the observations themselves.

1.2.2 Calibrator Observation Selection

The density of good position calibrators on the sky is insufficient that only sources with very good SNR can be used. To get a sufficient density of measurements for a distortion calibration, measurements with an SNR of a few must frequently be used. This is very prone to false detections especially when very bright sources with prominent sidelobes are in the field of view. A further complication is that ionospheric position shifts can be very large (10's of arcmin at 74 MHz) so that a large field around each potential calibrator must be searched. Yet another complication is that when the catalog, typically NVSS, is at a very different frequency and resolution, it is not possible to tell which of the potential sources will actually be detectable. These all increase the likelihood of false detections.

For each snapshot calibrator observation, if the peak in the allowed search area is above a specified threshold, the centroid of the source, the peak intensity and an integrated measurement of the flux density in the region of the peak is determined. Selection of valid calibrator measurements involves a number of filtering steps. The following describe the filtering implemented in the Obit package tasks IonCal and IonImage.

Heavily resolved sources and side–lobes can frequently be detected by a comparison of the peak and integrated flux densities. Any measurement in which the integrated value is less that a third or more than three times the peak is rejected. The next level of filtering is to make a preliminary fit of the Zernike model and restrict the measurements to those which do not grossly differ from the model. All fits are weighted by the peak flux density. Subsequent processing uses all position offset measurements derived from the entire dataset. An initial Zernike fit is made to each time segment and the residual from the model determined for each measurement. If the calibrator catalog is at a very different resolution or frequency, the cataloged position may not the the appropriate one for partially resolved sources. Each source is examined for systematic offsets from the cataloged position and if these are sufficiently large, an constant offset is added to the cataloged position.

A critical parameter for the filtering process is a target RMS residual, essentially the residual "seeing" size that is allowed. The residuals of each measurement are compared with the target residual and measurements with excessive residuals are rejected. The fits to the individual time segments are recomputed and if the RMS is excessive, the most discrepant point is rejected. This is repeated until either the RMS residual is acceptable or there are too few measurements for a fit. In the latter case, this time segment is flagged and excluded from further imaging. A global RMS residual is computed and reported as the "seeing"; note, this is a Gaussian sigma, not a FWHM (2.35 times larger).

1.2.3 Temporal Editing

The ionosphere can be extremely variable and the times of the most disturbed conditions should be excluded from imaging. Times of disturbed conditions are usually indicated by defocusing; in extreme cases, none of the calibrators are detected so no fit is possible. The RMS residuals from

the relatively simple model may also be unacceptable causing the time segment to be rejected. In less extreme cases, defocusing can be detected from the peak values of the calibrators. For each calibrator, the average image peak is determined. If in any time segment, the average ratio of the calibrator peak to its average drops below a given threshold, the time segment is rejected.

1.2.4 Cases when Field–Based Calibration is Inappropriate

If the isoplanatic patch size is larger than the field of view, then traditional self–calibration is a better approach. At the other extreme, if there are significant deviations from a linear phase gradient across the array for a wavefront from a given source, then sources will be defocused and field–based calibration cannot correct this. In the limit of very large higher order phase perturbations, the calibrator images will be completely defocused and image plane calibration techniques are not applicable.

1.2.5 Ionospheric Phase Screen Model

Currently, a Zernike polynomial is used as the parameterized model of the ionosphere. At low order, this parameterization is adequate and for the VLA at 74 MHz, there are seldom enough detectable calibrators to justify more than a 5 term Zernike polynomial. At higher order, the Zernike polynomials are less effective. They have trouble representing actual phase screens and share the general problem of polynomial fitting that they can become unstable and produce wild values where not well constrained. A better behaved parameterized model of the ionospheric phase screen is needed.

1.2.6 Other Errors

Not all of the corruptions of data are the result of the ionosphere. Another likely cause is the non circularity of the antenna patterns. If a source is far from the pointing center and is observed with a non-circularly symmetric, alt-az mounted antenna, the gain in the direction of the source will be time variable. For a sufficiently strong source, this will produce visible artifacts in the image.

1.2.7 Example

Examples of field–based calibration are shown in Figures 1.3 and 1.4. The data being calibrated were VLA observations at 74 MHz in B configuration. The calibration used 2 minute solutions on calibrators stronger than 3 Jy. The left column of these figures show the time sequence of observed source offsets as a function of location in the field of view. The right column show the residuals after selection, fitting a 5 term Zernike model and subtracting the model. As can be seen from these figures, the model fitting makes a significant improvement in the residuals but does not always completely remove the systematics.

1.3 Wide–field Imaging with a Fly's Eye and Catalog

The technique used for wide–field imaging of low frequency observations applying field–based calibration proceeds as follows. The imaging in Obit manipulates image mosaics using class ObitImageMosaic. A field of view is specified which is the radius from the pointing center of to be completely imaged. The data is examined and the cells spacing (if not specified) is picked on the basis of the longest baseline in the data and the size of a facet "undistorted" by coplanarity effects determined from the maximum w in the selected data. A "Fly's Eye" tessellation of round regions in a hexagonal pattern is then defined which fully covers the field of view and a set of square images enclosing these circular regions is added to the mosaic. At 74 MHz the Fly's Eye of the full VLA beam will include hundreds to thousands of facets.

In general, the imaged field of view does not enclose all of the sky to which the array elements have non–zero gain, so there is the possibility of sources visible outside of the fully imaged field of

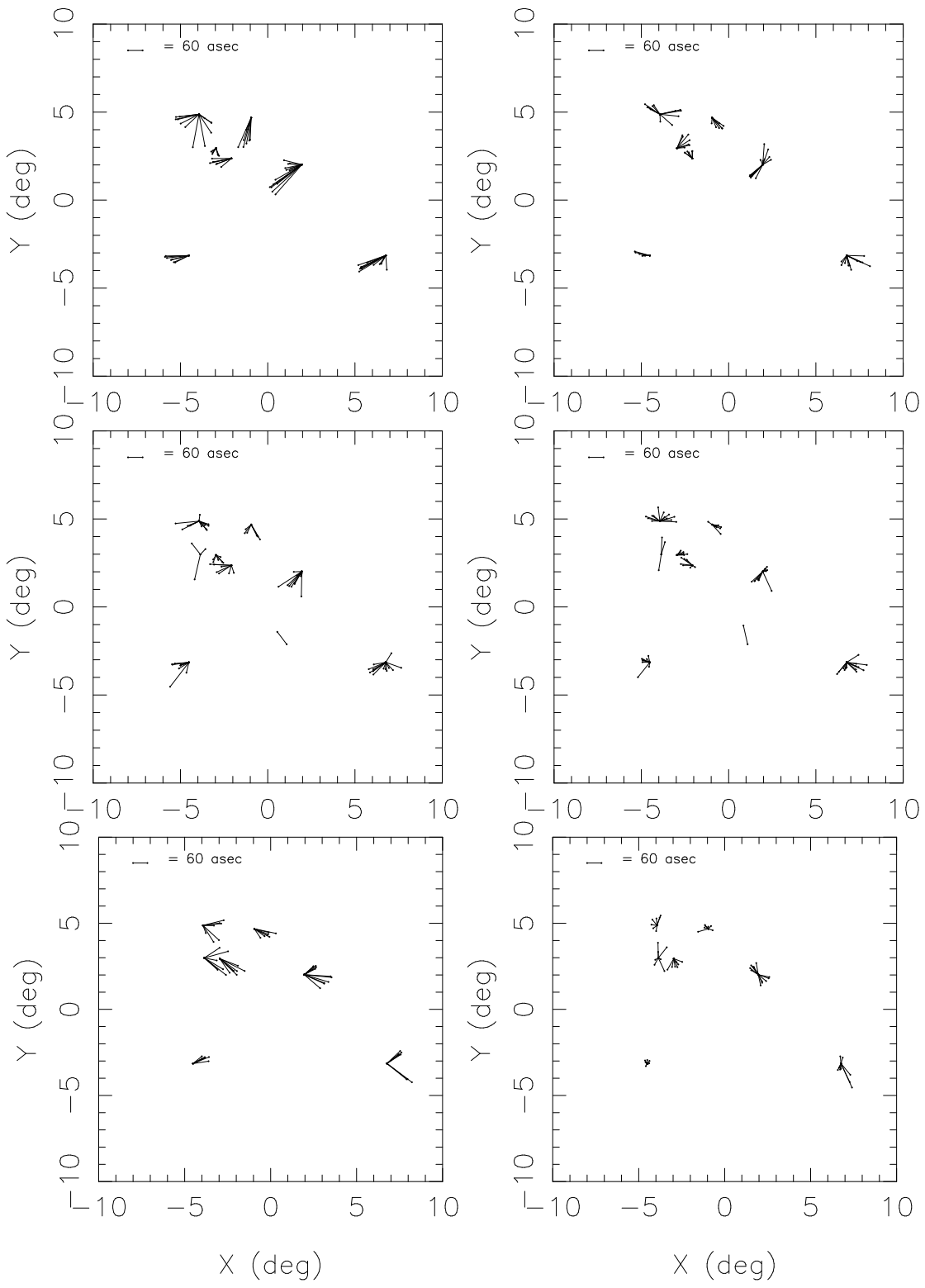

Figure 1.3: Sequences of apparent calibrator offsets as a function of time and location in the field of view. The length of each vector is 50 times the actual apparent displacement. Each set of vectors represents the measured offsets in a given solution interval with 7 sets of contigious time samples per panel. On the left are the observed offsets and on the right are the corresponding residuals after fitting and removing a 5 term Zernike model.

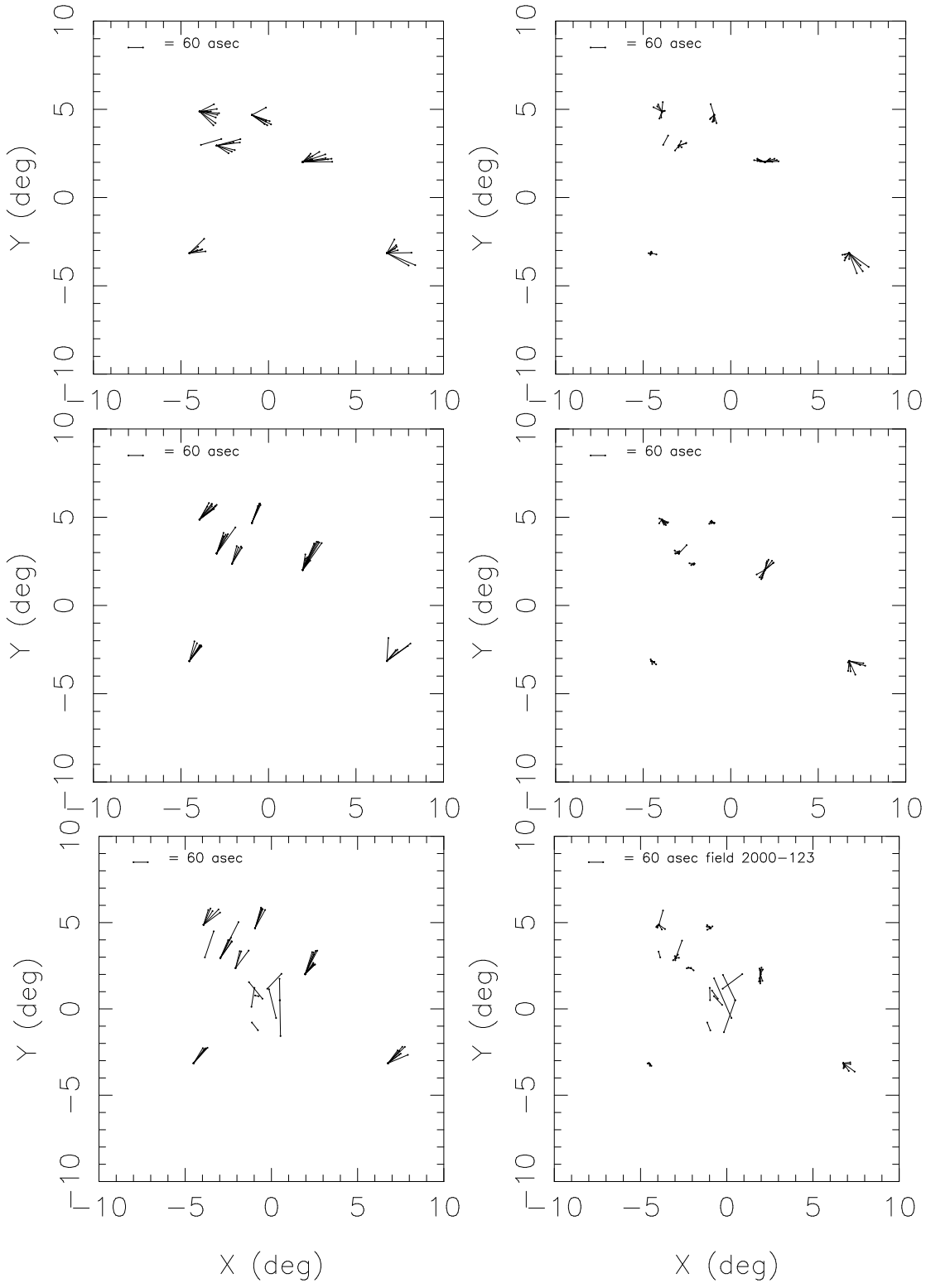

Figure 1.4: Similar to Figure 1.3 but for subsequent time samples.

view. To include such sources, facets are added to the mosaic centered on the positions of outlying sources from a catalog (currently a stripped down version of the NVSS) which are deemed to have an apparent brightness above a given threshold based on a given spectral index and a model of the antenna pattern.

To correct for the ionospheric model in the image formation, the phase for each antenna is evaluated from the field–based ionospheric model as a time series at the center of each facet. This calibration is then applied to the data prior to forming the image. This process is repeated for each facet and for each residual image calculation. Given an accurate model of the ionosphere, this technique could correct for an arbitrarily complex ionosphere.

Following the "OVERLAP 2" method of AIPS, all facets in the mosaic are formed and a quality measure based on both peak brightness and extended emission is used to determine which facet is to be CLEANed first. Components are selected from this facet and then subtracted from the visibility data. The next highest quality measure facet is re-imaged and if it is still the highest quality facet, it is CLEANed, otherwise, the next highest facet is re-imaged and tested, etc.

The subtraction of the dedistorted CLEAN model from the observations of the distorted sky requires a time variable redistortion of the image. This process involves the same approximation used in field–based calibration, the sources are only shifted in apparent position and not distorted. The list of components being subtracted have a time variable apparent position shift applied. The position shift is computed at the actual celestial position of the component at the times of data from which the model is being subtracted. This involves a "DFT", a direct Fourier transform, in which the effect of each component for a given visibility is calculated and then summed over component.

After the CLEAN is finished, components are (optionally) restored to the facet from which they were subtracted as well as to any overlapping facet in which their position appears. After restoration of the subtracted components, all facets are projected ("flattened") onto a grid covering the specified field of view.

1.4 Peeling

Bright sources can be particularly troublesome. Even under relatively quiessent conditions ionospheric phase fluctuations are large enough that unusually bright sources introduce artifacts into the images produced. A technique labeled "Peeling" ("the onion") has been developed for this case. A self calibration of the source followed by a subtraction of the derived source model followed by a reversal of the effects of the self–calibration can remove the effects of the source to a large degree. The details of this technique as implemented in Obit task IonImage are described in the following.

Following a field–based calibration, the initial set of facet images are made. If the autoCenter feature is enabled, an initial imaging followed by a subsequent imaging with the bright sources centered on a pixel at the center of a facet is performed. If the brightest pixel in any facet exceeds the peeling threshold, a shallower than normal CLEAN is performed (to 0.1 of the peeling threshold). Since the residual images are not needed, the full set is not recomputed at the termination of the CLEAN. Then the model of all the fields except the one to be peeled are then subtracted from the data using the field–based calibration. This should remove most of the effect of other sources in the field such that this residual data set is dominated by the source to be peeled. This residual data set is then used to phase self–calibrate the source to be peeled. The self–calibration solution is then applied to the original data and the self–calibrated model subtracted. An inverse of the phase self calibration calibration is then applied to the data. This leaves the data with the strong source largely removed. The CLEAN components defining the model of the peeled source are copied to a table which is not used by subsequent processing. The normal field–based imaging and deconvolution then proceeds. When the deconvolution is complete, the CLEAN components from the peeled model are copied to the corresponding table on the facet from which the peeled source was removed. Thus, when the components are restored to the images and the final image flattened, the model used to peel the strong source is included.

An example of the results of peeling is shown in Figure 1.5. This data was made with the VLA

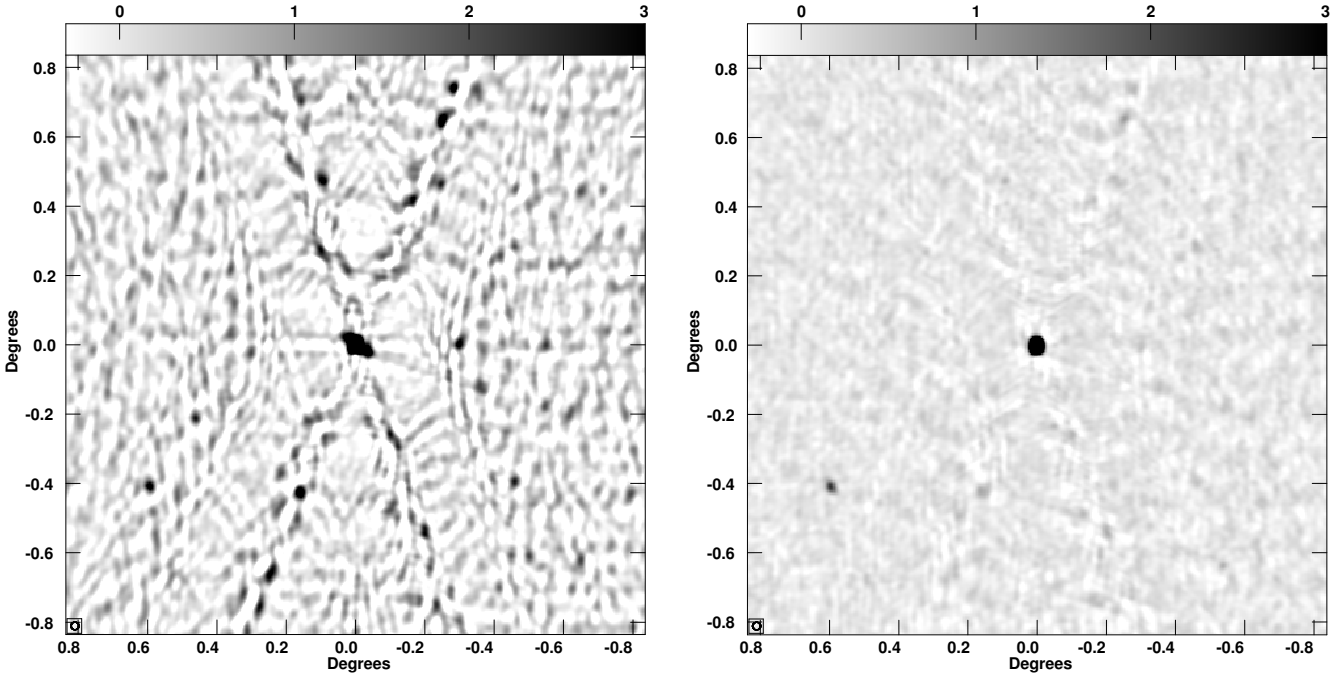

Figure 1.5: Example of peeling a strong source. On the left is the result of applying only the field–based calibration to the field around a strong calibrator, shown in reverse grayscale with a scale wedge at the top (labeled in Jy). The resolution is indicated in the lower left. On the right is the same field after applying field–based calibration and peeling the source.

at 74 MHz in the B configuration. There is a dramatic difference in the quality of the images; the deconvolution of the unpeeled image spent most of its CLEANing on artifacts and didn't even properly deconvolve weaker sources. The peak in the image made with peeling was 30.4 Jy/beam with a full field RMS of 96 mJy whereas the unpeeled image had a peak of 31.0 Jy/beam and an RMS of 223 mJy/beam.

1.5 Discussion

This document describes low frequency calibration and imaging techniques which are successful for imaging VLA 74 MHz B configuration data under relatively typical circumstances. Several examples derived from observations are presented. These techniques need further development for longer baselines or lower frequencies. A technique of peeling strong sources is shown to significantly improve the derived image.

Bibliography

[1] W. D. Cotton. Lessons from the VLA Long Wavelength Sky Survey (VLSS). In *Science with Human Wavelengths, Astronomical Society of the Pacific Conference Series, vol, 345*, pages 337–340, 2005.

[2] W. D. Cotton, J. J. Condon, R. A. Perley, N. Kassim, J. Lazio, A. Cohen, W. Lane, and W. C. Erickson. Beyond the isoplanatic patch in the VLA Low-frequency Sky Survey. In *Proceedings of the SPIE, Volume 5489.*, pages 180–189, 2004.

[3] W. D. Cotton and J. M. Uson. Ionospheric Effects and Calibration of the VLA at 327 MHz. *EVLA Memo 117*, ftp://ftp.cv.nrao.edu/NRAO-staff/bcotton/Obit/Ion327.pdf:1–12, 2007.